Behavioral and histopathological consequences of paraquat intoxication in mice: Effects of α-synuclein over-expression

7 **AUTHORS**, INCLUDING:

Pierre-Olivier Fernagut

Université Victor Segalen Bordeaux 2

65 PUBLICATIONS **2,195** CITATIONS

SEE PROFILE

Nicole A. Tetreault

Gifted Research and Outreach

12 PUBLICATIONS **749** CITATIONS

SEE PROFILE

Behavioral and Histopathological Consequences of Paraquat Intoxication in Mice: Effects of α-Synuclein Over-Expression

P.O. FERNAGUT,[1,2] C.B. HUTSON,[1,2] S.M. FLEMING,[1,2] N.A. TETREAUT,[1,2] J. SALCEDO,[1,2]
E. MASLIAH,[3] AND M.F. CHESSELET[1,2*]
[1]Department of Neurology, The David Geffen School of Medicine at UCLA, Los Angeles, California 90095-1769
[2]Department of Neurobiology, The David Geffen School of Medicine at UCLA, Los Angeles, California 90095-1769
[3]Department of Neuroscience, Univeristy of California, San Diego, La Jolla, California 92093-0624

ABSTRACT   Genetic variability in the α-synuclein gene and long-term exposure to the pesticide paraquat constitute possible risk factors for sporadic Parkinson's disease. The goal of the present study was to further characterize the effects of paraquat in mice as a model of Parkinson's disease and to determine whether it acted synergistically with α-synuclein over-expression to cause nigrostriatal cell death or dysfunction. Paraquat (10 mg/kg i.p.) was administered once a week for 3 weeks to mice over-expressing human α-synuclein under the Thy1 promoter and their wild-type littermates. The effect of paraquat on catecholaminergic neurons was reminiscent of that of Parkinson's disease, with preferential loss of dopaminergic neurons in the ventral tier of the substantia nigra pars compacta and loss of tyrosine hydroxylase staining in the locus coeruleus. α-Synuclein over-expression did not increase paraquat-induced cell loss, and paraquat did not worsen the behavioral deficits observed in the transgenic mice. However, paraquat markedly increased proteinase-K-resistant α-synuclein aggregates in substantia nigra of the transgenic mice. The data further validate the use of paraquat to model Parkinson's disease in mice and show that although paraquat and α-synuclein over-expression act synergistically to increase protein aggregation in vivo, this interaction does not result in short-term neuroprotection or increased vulnerability of nigrostriatal neurons. **Synapse 61:991–1001, 2007.**   © 2007 Wiley-Liss, Inc.

INTRODUCTION

Parkinson's disease (PD) is a prevalent neurodegenerative disorder, affecting 1–2% of the population over 65 years old. Despite the identification of several genes causing familial PD, the causes of the much more frequent sporadic forms of PD remain elusive. One protein involved in familial PD, α-synuclein, may also contribute to the pathophysiology of the sporadic forms. Indeed, α-synuclein is a component of Lewy bodies, the cytoplasmic aggregates present in neurons of the central and peripheral nervous system in sporadic PD (Braak et al., 2003). Furthermore, α-synuclein gene haplotypes that increase the levels of this protein are a risk factor for sporadic PD (Farrer et al., 2001; Holzmann et al., 2003; Pals et al., 2004).

Together with genetic risk factors, environmental exposure may play a role in sporadic PD (Di Monte et al., 2002; Greenamyre and Hastings, 2004). In particular, long term exposure to the herbicide paraquat (1,1′-dimethyl-4,4′-bipyridinium) increases the risk of PD (Hertzman et al., 1990; Liou et al., 1997; Semchuk et al., 1992). Supporting a toxic effect of paraquat on dopaminergic neurons, systemic adminis-

tration of this pesticide kills a subset of nigrostriatal dopaminergic neurons in mice (McCormack et al., 2002, 2005). It is unknown whether the dopaminergic neurons affected by paraquat are those most vulnerable in PD, and whether the toxin affects other regions also affected in PD, such as the locus coeruleus (LC) (Halliday et al., 1990; Jellinger, 1991). Furthermore, it is not clear whether α-synuclein and paraquat act synergistically to cause dopamine cell loss. Previous studies have shown that paraquat increases α-synuclein fibrillation in vitro and induces the formation of α-synuclein aggregates in vivo (Manning-Bog et al., 2002). However, a resistance to paraquat-induced cell loss was observed in mice with a low level of α-synuclein over-expression in catecholaminergic neurons (Manning-Bog et al., 2003). Yet others have found an increased cell loss in α-synuclein over-expressors when paraquat was administered with maneb in another line of mice with more severe α-synuclein pathology (Thiruchelvam et al., 2004).

A first goal of the present study was to further validate the use of paraquat to model PD in mice by determining whether paraquat-induced cell loss resembles that seen in PD. Specifically, we sought to identify the pattern of TH cell loss within the substantia nigra pars compacta and to examine paraquat effects on LC neurons. A second goal was to determine whether paraquat and α-synuclein over-expression act in synergy in a well characterized mouse model of α-synuclein over-expression. In these mice, expression of human wild-type α-synuclein is driven by the Thy-1 promoter (Rockenstein et al., 2002), resulting in broad over-expression throughout the brain and the formation of proteinase-K-resistant aggregates of α-synuclein. These mice display progressive sensorimotor anomalies in behavioral tests sensitive to nigrostriatal dysfunction, altered response to dopaminergic drugs, alterations in striatal dopamine receptor function, and olfactory deficits (Fleming et al., 2004, 2006a,b; Wu et al., 2005). We investigated whether paraquat-induced cell death was altered by α-synuclein over-expression in these mice. In addition, we have used a battery of sensitive behavioral tests previously shown to detect anomalies caused by nigrostriatal dopamine loss (Hwang et al., 2005) to determine (1) whether the small nigrostriatal dopamine cell loss induced by paraquat results in behavioral deficits, and (2) whether paraquat worsened behavioral deficits and α-synuclein pathology in these mice.

MATERIAL AND METHODS
Animals and paraquat administration

Mice over-expressing human wild-type α-synuclein under the Thy-1 promoter (Thy1-aSYN) were created previously (line 61, Rockenstein et al., 2002) and maintained on a mixed C57BL/6-DBA/2 background. Male Thy1-aSYN ($n = 14$) and their wild type (WT) littermate ($n = 14$) aged 12–14 weeks at the beginning of the experiment were used. Animal care was conducted in accordance with the United States Public Health Service *Guide for the Care and Use of Laboratory Animals*, and procedures were approved by the University of California Los Angeles Institutional Animal Care and Use Committee. Seven litters were used in the present study. Wild-type littermates and transgenic mice from each litter were carefully balanced in all groups. Mice were divided into four groups: WT + saline ($n = 7$), WT + paraquat ($n = 7$), Thy1-aSYN + saline ($n = 7$), and Thy1-aSYN + paraquat ($n = 7$). Paraquat dichloride (Sigma) was dissolved in 0.9% NaCl to a final concentration of 1 mg/ml and freshly prepared before each injection. Mice received 3 i.p. injections of either paraquat (10 mg/kg) or vehicle (0.9% NaCl) 1 week apart and were killed 5 days after the last injection.

Behavioral assessment
Challenging beam traversal

The challenging beam traversal test was performed as previously described (Fleming et al., 2004). The plexiglas beam (Plastics Zone, Woodland Hills, CA) was made of four sections (25 cm length) starting at a width of 3.5 cm and gradually narrowing to 0.5 cm × 1 cm increments. Animals were trained to traverse the beam starting at the widest section and ending at the narrowest section, which led directly into the animal's home cage. Animals were trained for 2 days before testing, each training session consisting of five trials. On the day of the test, a mesh grid (1 cm^2) of corresponding width was placed over each segment of the beam, leaving a 1-cm space between the grid and the beam surface. Animals were videotaped while traversing the grid-surfaced beam for a total of five trials. The challenging beam traversal test was performed at baseline and then 3 days after the last paraquat injection. Videotapes were rated for number of errors, number of steps and time to traverse by an investigator blind to the animal genotype and treatment.

Pole test

The pole test was performed according to Matsuura et al. (1997) with minor modifications (Fleming et al., 2004). The mouse was placed head upward on the top of a vertical wooden rough-surfaced pole (diameter: 1 cm, height: 50 cm). Each mouse was habituated to the apparatus for 2 days prior to testing, then allowed to descend five times. The total time until the mouse reached the floor with its forepaws was recorded (T-total) as well as the time needed for the mouse to turn completely head downward (T-turn). For each

session of five descents, the best performance was kept for the T-turn and T-total. If the mouse was unable to turn completely downwards, fell or slipped down, the default value 60 s for T-Turn and 120 s for T-total were taken into account. The pole test was performed at baseline and 3 days after the last paraquat injection.

Histopathological analysis

Tissue processing

Five days following the last paraquat injection, mice were anesthetized with pentobarbital (100 mg/kg i.p.) and intracardially perfused with 0.1 M PBS followed by ice cold 4% paraformaldehyde (PFA). Brains were quickly removed, postfixed for 2 h in 4% PFA, then cryoprotected in 30% sucrose in 0.1 M PBS, frozen on powdered dry ice and stored at $-80°C$. Forty-micrometer free-floating coronal sections were collected for histopathological analysis

Immunohistochemistry

Sections were washed in 0.1 M PBS (pH = 7.4) and incubated with 0.3% hydrogen peroxide for 15 min to block endogenous peroxidases. After washing in PBS, sections were incubated for 1 h in 10% normal goat serum/0.3% triton X-100 in PBS then incubated overnight at 4°C in the primary antibody with 2% normal goat serum: rabbit anti tyrosine hydroxylase (1/800, Pel Freez, Rogers, Arkansas), rat anti CD-68, a marker of microglial cells (1/500, Serotec, Raleigh, NC). After washing in PBS, sections were incubated with the corresponding biotynilated secondary antibody, either goat anti-rabbit IgG (1/1000, ICN Biomedical, Irvine, CA) or goat anti-rat IgG (1/500, ICN Biomedical, Irvine, CA) at room temperature for 2 h. The avidin-biotin complex method was used to detect the secondary antibody (ABC elite kit, Vector laboratories, Burlingame, CA) and the reaction product was visualized by 3,3′-diaminobenzidine tetrachloride (DAB, Sigma).

For α-synuclein immunohistochemistry, sections were first washed in PBS, and then incubated in PBS containing 10 μg/ml proteinase-K (Invitrogen, Carlsbad, CA) for 10 min at room temperature. After washing in PBS (3 × 10 min), sections were incubated in mouse on mouse blocking solution (MOM kit, Vector Laboratories, Burlingame, CA) for 1 h then incubated overnight at 4°C with monoclonal mouse anti-α-synuclein (610787, formerly Transduction laboratories S63320, 4 μl/ml, BD Biosciences, San Jose, CA), which recognizes both mouse and human α-synuclein (van der Putten et al., 2000). Control sections incubated with either no primary antibody or mouse IgG$_1$ (4 μl/ml, Sigma) were devoid of immunoreactivity. Specificity of the antibody was also assessed by west-

ern immunoblot, and detected a band at the expected molecular weight of 19 kDa (data not shown). Sections were then washed in PBS, and incubated with the secondary antibody (biotynilated goat anti-mouse IgG F (ab)$_2$, 1/500; ICN Biomedical, Irvine, CA) The avidin–biotin complex method was used to detect the secondary antibody (ABC elite kit, Vector laboratories, Burlingame, CA) and the reaction product was visualized by DAB (Sigma). For all immunoreactions, control sections were incubated with either no primary antibody or with the corresponding IgG at the same concentration as the primary antibody.

Measurement of TH fiber density and optical density in the striatum

To evaluate the effects of paraquat on striatal dopaminergic terminals, TH immunostained striatal sections were analyzed using two different methods: TH-OD, a densitometric measurement assessing the averaged intensity of immunostaining in the region examined and TH fiber density, which measures the surface area occupied by TH positive fibers in the region examined.

Fiber density was measured in the striatum at Bregma +0.98 mm with a computer assisted image analysis system, using NIH image v 1.32 as previously described (Bordelon and Chesselet, 1999). Anatomical landmarks (aspect, size, and position of the anterior commissures, corpus callosum, septum, lateral ventricles, striatum, and nucleus accumbens) were used to ensure that TH-IR was analyzed at similar levels within and between groups and immunoreactions were carefully controlled to avoid variations in staining intensity. Sections were examined on a Zeiss Universal microscope with a 16× objective. After calibration of the system to ensure adequate exposure and avoid saturation of gray levels, images were captured using an Oscar CCD camera (Techni-Quip, El Segundo, CA). Threshold for detection of specific TH-immunolabeling was set in the corpus callosum. TH fiber density was then determined in a 75 μm × 75 μm area. The area was placed so that myelinated fibers that cross the striatum were carefully excluded from measurements. Measurements were performed in the dorsolateral, dorsomedial, ventrolateral, and ventromedial part of the striatum. Measures were performed on the left and right striatum and averaged.

Optical density (OD) measurements of tyrosine hydroxylase immunoreactivity (TH-IR) were performed with a computer assisted image analysis system (Spot camera equipped with 55-mm micro Nikkor lens f/2.8, ImageJ v1.32). Images were acquired after calibration of the system to ensure adequate exposure and avoid saturation of gray levels. Regions of interest (striatum and adjacent cortex) were delineated as follows: the outer border of the striatum was defined

by the lateral ventricle medially, the corpus callosum dorsally and laterally, and by a line drawn between the two anterior commissures ventrally, whereas the adjacent cortex was defined ventrally by the corpus callosum. After subtraction of the nonspecific staining, the TH-IR OD was measured in the striatum and the adjacent sensorimotor cortex. Because TH-IR fibers are very sparse in the cortex, the value in cortex was considered a blank and was used to normalize staining levels for each section. Accordingly, reported TH-OD values in striatum represent the difference between TH-OD measured in striatum and cortex. Measurements were performed on the whole striatum then in the dorsolateral, dorsomedial, ventrolateral, and ventromedial parts. Measures were performed on the left and right side and averaged for each section.

Histopathological analysis

For the substantia nigra pars compacta (SNc), every fourth section was processed for TH-IR. Stereological sampling was performed using the Stereo Investigator software (MicroBrightField, Colchester, VT) coupled to a Leica DM-LB microscope with a Ludl XYZ motorized stage and z-axis microcator (MT12, Heidenheim, Traunreut, Germany). Following delineation of the SNc at 5× objective as described by McCormack et al. (2002) to ensure anatomical accuracy and adequate number of sampling sites in the whole SNc and subdivisions, counting was performed at 100× objective. Guard zones of 1.5 μm ensured the exclusion of lost profiles on the top and bottom of the section sampled. To determine if there may exist a differential neuronal vulnerability to paraquat within the SNc, stereological cell counting were performed on several subdivisions of the SNc defined according to known patterns of dopamine transporter or calbindin D-28K expression, or neuronal vulnerability established in weaver mutant or MPTP-treated mice (Graybiel et al., 1990; Liang et al., 1996; Sanghera et al., 1997). After delineating the whole SNc, two regions corresponding to the 250 μm medial part (e.g., next to the ventral tegmental area) and lateral part (e.g., next to the external tip of the cerebral peduncle) were outlined. The central part lying in between the medial and lateral portion was then further divided by outlining a ventral region corresponding to one-third of the size of this central part (Fig. 2A). These criteria were used at every level and were chosen to isolate for analysis subregions, which have been shown to display differential vulnerability in PD and after other toxicants, such as MPTP.

For the LC, every other section was stained for TH immunohistochemistry and counterstained with cresyl violet, resulting in six sections sampled per mouse. The number of neurons in the SNc and LC was estimated using the optical fractionator method, which is unaffected by changes in the volume of reference of the structure sampled and is thus suitable to estimate the number of neurons in brain nuclei that lack well defined anatomical boundaries.

The estimated total number of TH-IR neurons in the substantia nigra and the LC was calculated based on the following formula: $N = Q^- \times 1/\text{ssf} \times 1/\text{asf} \times t/h$ (West et al., 1991), where N is the estimate of the total number of cells, Q^- is the number of objects counted, ssf is the section sampling fraction, asf is the area sampling fraction, and t/h is the actual section thickness divided by the height of the dissector. Between 150 (SNc subregions, LC) and 300 objects (whole SNc) were counted to generate the stereological estimates. Gundersen coefficients of error were less than 0.1.

α-Synuclein immunoreactive inclusions and CD-68 immunoreactive microglial cell were counted at the mid-nigral level (Bregma −3.16 mm). The whole substantia nigra was delineated using anatomical landmarks (tips of the cerebral peduncles, medial terminal nuclei of the accessory optic tract). Inclusions were counted on two sections on the left and right substantia nigra then averaged for each mouse. Measurements of the diameter of the inclusions were performed on 30 randomly selected inclusions for each mouse. All cell counts were performed by an investigator blind to the animal genotype and treatment.

Statistical analysis

Histopathological data were analyzed using a two-way ANOVA with genotype and treatment as independent variables. Behavioral data were analyzed using a two-way ANOVA with repeated measures comparing pre- and postintoxication performances. Post hoc analysis was performed with Fisher's LSD test. Comparison of α-synuclein inclusions between vehicle and paraquat-treated Thy1-aSYN mice was performed with Student t-test. Statistical analysis was performed with GB-STAT v8.0 (Dynamic microsystems, Silver Springs, MD). For all statistical tests, the level of significance was set at $P < 0.05$.

RESULTS
Survival and behavior

The transgenic mice used in this study (Thy1-aSYN) over-express human wild-type α-synuclein broadly in brain under the Thy1 promoter (Rockenstein et al., 2002). Only one Thy1-aSYN mouse died during paraquat administration, immediately after the second injection. There was no effect of paraquat on body weight, and no overt signs of systemic toxicity were observed during the study.

As previously reported (Fleming et al., 2004), behavioral assessment of sensorimotor function revealed
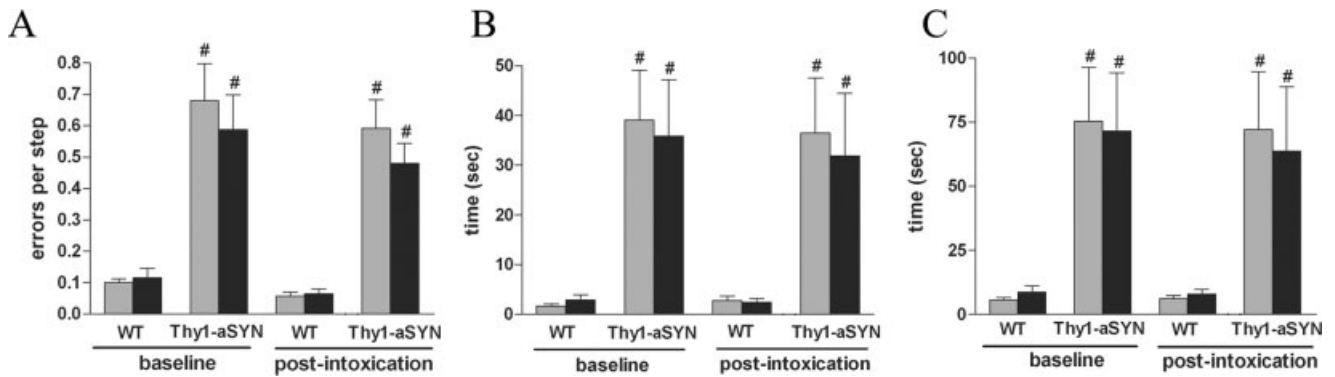
Fig. 1. Behavioral assessment before and after administration of saline (grey bars) or paraquat (black bars) in WT and α-synuclein over-expressing mice (Thy1-aSYN). **A**: Errors per step on the challenging Beam. **B**, **C**: Time to orient downward (T-Turn, B) and descend (T-Total, C) on the pole test. #, $P < 0.01$ compared with WT mice using two-way ANOVA with repeated measures followed by Fisher's LSD test, $n = 6$–7 mice per group.

TABLE I. *Tyrosine hydroxylase immunoreactivity optical density (OD)*
and fiber density (FD) in the striatum

		WT saline	WT paraquat	Thy1-aSYN saline	Thy1-aSYN paraquat
Striatum	OD	0.1167 ± 0.008	0.1019 ± 0.007	0.1202 ± 0.009	0.1013 ± 0.01
DL	OD	0.1247 ± 0.009	0.1094 ± 0.009	0.1181 ± 0.007	0.1066 ± 0.012
	FD	1615 ± 98.87	1419 ± 161.6*	1579 ± 92.34	1279 ± 55.24*
DM	OD	0.1128 ± 0.012	0.0977 ± 0.008	0,1090 ± 0.007	0.095 ± 0.011
	FD	1449 ± 86.87	1181 ± 94.17**#	1430 ± 43.10	1079 ± 55.05**##
VL	OD	0.1237 ± 0.007	0.1058 ± 0.008	0.1211 ± 0.009	0.1031 ± 0.01
	FD	1354 ± 65.62	1180 ± 103	1368 ± 86.61	1177 ± 83.83
VM	OD	0.1032 ± 0.009	0.091 ± 0.006	0.1132 ± 0.006	0.096 ± 0.009
	FD	1177 ± 78.96	1044 ± 63.23*	1147 ± 51.92	1017 ± 34.27*

DL, dorsolateral; DM, dorsomedian; VL, ventrolateral; VM, ventromedian.
*$P < 0.05$,
**$P < 0.001$, significant effect of treatment using two-way ANOVA.
#$P < 0.05$, ##$P < 0.01$ compared with corresponding saline group using two-way ANOVA followed by Fisher's LSD test, $n = 6$–7 mice per group.

impaired performance of Thy1-aSYN mice. On the beam traversal task, there was a significant effect of genotype ($F_{(1,55)} = 79.96$, $P < 0.0001$) and Thy1-aSYN mice made significantly more errors per step than their WT counterparts ($P < 0.01$, Fig. 1A). ANOVA also revealed an effect of genotype for time to traverse the beam ($F_{(1,55)} = 4.94$, $P < 0.05$). Post hoc analysis indicated that Thy1-aSYN mice took significantly more time to traverse the beam (21.93 ± 5.39 vs. 10.06 ± 1.2 s, $P < 0.05$). Thy1-aSYN mice occasionally displayed freezing episodes when entering the narrowest segment of the beam. Paraquat administration did not increase the time to traverse or the number of errors in Thy1-aSYN and WT mice. Prior to paraquat intoxication, Thy1-aSYN mice also displayed a significant deficit on the pole test (Figs. 1B and 1C). ANOVA indicated a significant effect of genotype for T-Turn, ($F_{(1,55)} = 21.002$, $P < 0.0001$) and T-Total ($F_{(1,55)} = 18.38$, $P = 0.0003$). Thy1-aSYN mice took significantly longer to fully orient downward (T-Turn, $P < 0.01$), and to descend the pole (T-total, $P < 0.01$), demonstrating impaired postural adjustments and frequent sliding when attempting to orient down-

ward. These impairments in the pole test were unchanged after paraquat administration.

Histopathology

Effect of paraquat on striatal dopaminergic terminals

Dopaminergic terminals in the striatum were analyzed using two different methods. Both densitometric measurements (TH-OD) and assessments of the surface area occupied by TH positive fibers (fiber density) were performed on sections immunostained for TH (Table I). Measurements of TH-OD in the striatum revealed a small decrease in paraquat treated Thy1-aSYN and WT (-15.8% and -12.7%, respectively) that failed to reach significance ($F_{(1,25)} = 3.67$, $P = 0.068$). Measure of fiber density indicated a significant reduction in animals exposed to paraquat in the dorsomedial (DM, $F_{(1,25)} = 16.28$, $P < 0.001$), dorsolateral (DL, $F_{(1,25)} = 4.64$, $P < 0.05$) and ventromedial parts of the striatum (VM, $F_{(1,25)} = 4.37$, $P < 0.05$). The dorsomedial part of the striatum was the most
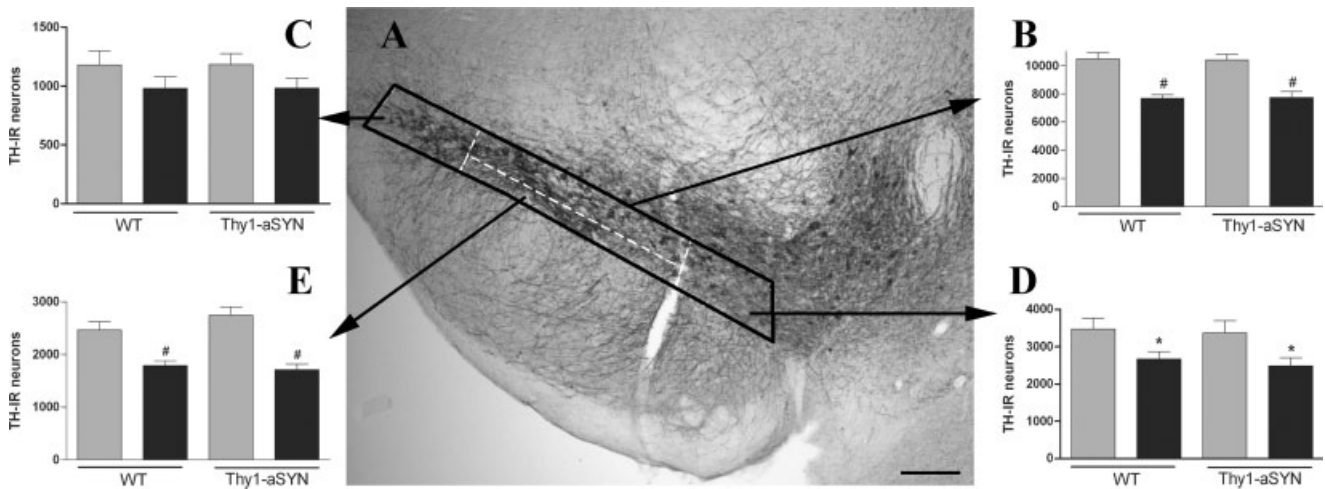
Fig. 2. Stereological counting of TH-IR neurons in the substantia nigra after administration of saline (grey bars) or paraquat (black bars) in WT and α-synuclein over-expressing mice (Thy1-aSYN). **A**: Illustration of subregions (white dashed lines) defined within the SNc (bold line). **B**: Stereological estimate in the whole SNc. **C**: Stereological estimate in the lateral part of the SNc. **D**: stereological estimate in the medial part of the SNc. **E**: Stereological estimate in the ventral part of the SNc. *, $P < 0.05$, #, $P < 0.01$ compared with corresponding saline group, using two-way ANOVA followed by Fisher's LSD test, $n = 6$–7 mice per group. Scale bar = 200 μm.

affected by paraquat exposure in WT (-18.5%, $P < 0.05$) and Thy1-aSYN mice (-25%, $P < 0.01$).

Stereological analysis in the substantia nigra and LC

Stereological estimate of the number of TH-IR neurons was performed in the whole SNc and in three subregions (lateral, medial and ventral, Fig. 2A). For the total number of TH-IR neurons in the SNc, two-way ANOVA indicated a significant effect of treatment ($F_{(1,25)} = 50.657$, $P < 0.0001$) but no effect of genotype or genotype X treatment interaction. Post hoc analysis using Fisher LSD test revealed that paraquat induced a significant decrease of the total number of TH-IR neurons in the SNc in both Thy1-aSYN (7740 ± 407 vs. $10,399 \pm 398$, -25.6%, $P < 0.01$) and WT (7673 ± 245 vs. $10,480 \pm 454$, -26.7%, $P < 0.01$) compared with their respective littermate controls (Fig. 2B). There was no difference in the number of TH-IR neurons in vehicle-treated Thy1-aSYN and WT mice. Stereological estimation of the number of TH-IR neurons in different subregions of the SNc revealed a nonhomogeneous pattern of TH-IR loss induced by paraquat. In the lateral part of the SNc, two-way ANOVA indicated a lack of significant effect of paraquat ($F_{(1,25)} = 3.75$, $P = 0.0657$, Fig. 2C). In the medial part of the SNc, paraquat induced a significant reduction of the number of TH-IR neurons ($F_{(1,25)} = 10.11$, $P < 0.01$). Post hoc analysis revealed a significant difference both in WT (-23.7%, $P < 0.05$) and Thy1-aSYN mice (-26.3%, $P < 0.05$, Fig. 2D). Among the three subregions analyzed, the ventral part of the SNc was the most affected by para-

quat ($F_{(1,25)} = 39.61$, $P < 0.0001$). Post hoc analysis indicated a significant reduction of the number of TH-IR neurons in WT (-30.4%, $P < 0.01$) and Thy1-aSYN mice (-37.6%, $P < 0.01$, Fig. 2E). No significant effect of genotype was detected in any of the regions sampled.

Histological analysis of the LC was performed on TH and Nissl stained sections using stereological cell counting procedures (Fig. 3). For TH-IR neurons, two-way ANOVA revealed a main effect of treatment ($F_{(1,25)} = 32.61$, $P < 0.0001$) but no significant effect of genotype or genotype X treatment interaction. Post hoc analysis using Fisher's LSD revealed that paraquat induced a significant decrease of the total number of TH-IR neurons in both Thy1-aSYN (-32.1%, $P < 0.01$) and WT mice (-26.2%, $P < 0.01$, Fig. 3A). ANOVA also revealed a slight but significant effect of paraquat on the number of Nissl stained neurons ($F_{(1,25)} = 5.04$, $P = 0.035$) indicating a moderate cell loss (-12% in WT mice and -14% in Thy1-aSYN), however no significant differences between groups were found by post hoc analysis using Fisher's LSD (Fig. 3B).

α-Synuclein immunohistochemistry

As previously reported (Rockenstein et al., 2002) sections from Thy1-aSYN mice that were not incubated with proteinase-K revealed intense immunostaining because of the presence of endogenous mouse α-synuclein and the sustained expression of the transgene. Aggregate-like structures could be observed but they were difficult to distinguish from the general high level of immunostaining (data not shown).
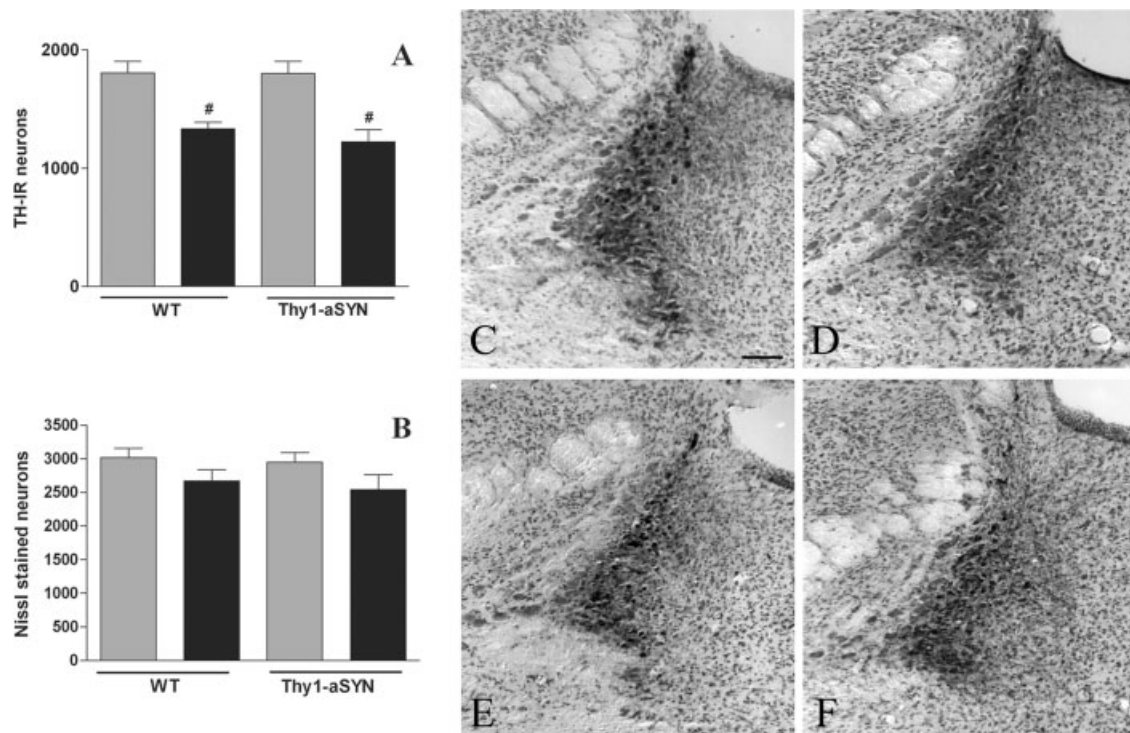
Fig. 3. Stereological estimate of the number of TH-IR neurons (**A**) and Nissl stained neurons (**B**) in the locus coeruleus after administration of saline (grey bars) or paraquat (black bars) in WT and α-synuclein over-expressing mice (Thy1-aSYN). #, $P < 0.01$ compared with corresponding saline group, using two-way ANOVA followed by Fisher's LSD test, $n = 6$–7 mice per group. Representative histological images of the locus coeruleus in saline-treated wild-type (**C**) or Thy1-aSYN mice (**D**) and paraquat-treated wild-type (**E**) and Thy1-aSYN mice (**F**). Scale bar = 200 μm.
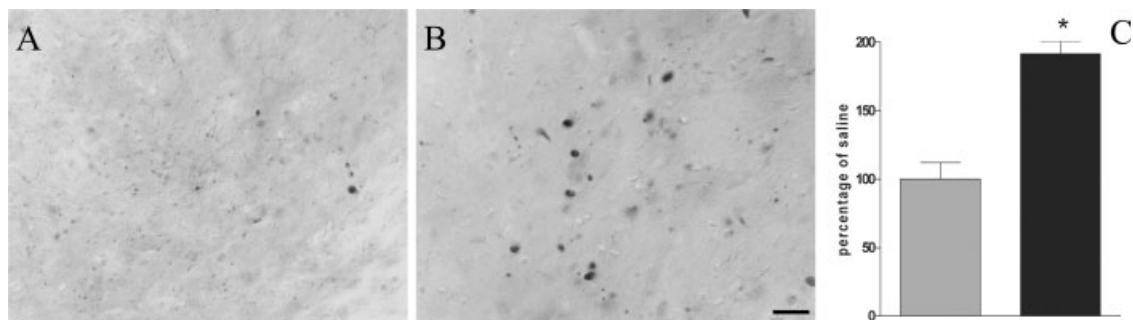

Fig. 4. Proteinase-K-resistant α-synuclein immunoreactive inclusions in the substantia nigra of a saline-treated (**A**) and paraquat-treated (**B**) Thy1-aSYN mouse. **C**: Increased the number of inclusions after administration of paraquat (black bar) compared with saline (grey bar). *, $P < 0.001$ compared with saline using student t-test, $n = 6$–7 mice per group. Scale bar = 20 μm.

Sections were subjected to a pretreatment with proteinase-K to selectively visualize insoluble α-synuclein. This treatment abolished immunostaining for endogenous α-synuclein in wild-type mice (data not shown) and revealed proteinase-K-resistant α-synuclein immunoreactive inclusions in many brain regions of the Thy1-aSYN mice (Hutson et al., in preparation), including the substantia nigra (Figs. 4A and 4B) and LC (not shown). Administration of paraquat induced a marked increase of the number of proteinase-K-resistant α-synuclein inclusions in the substantia nigra of Thy1-aSYN mice (+91.5%, $P < 0.001$, Fig. 4C). The diameter of these inclusions was also significantly increased in animals treated with paraquat (3.69 ± 0.18 μm vs. 3.01 ± 0.1 μm, $P < 0.01$). No difference was observed in the number of proteinase-K-resistant α-synuclein inclusions in the LC between saline and paraquat-treated mice. No proteinase-K-resistant α-synuclein inclusions were detected in saline or paraquat-treated WT mice with the antibody used in this study, which recognize both human and mouse α-synuclein. To determine whether the exposure to

paraquat and the subsequent increase of proteinase-K-resistant α-synuclein inclusions could be associated with an inflammatory response, adjacent midbrain sections were processed for CD-68 immunohistochemistry. No difference in the number of CD-68 positive cells was observed in any of the groups (data not shown).

DISCUSSION
Effects of paraquat on catecholaminergic neurons

We show that paraquat induces a 25% reduction of the number of TH-IR cells in the SNc. This is consistent with the result of previous studies, which established that the decrease in TH-IR neurons induced by paraquat in the SNc is due to a loss of neurons (Manning-Bog et al., 2003; McCormack et al., 2002, 2005). The partial loss of TH-IR neurons in the SNc after paraquat suggests that a sub-population of dopaminergic neurons may be particularly vulnerable to this toxin (McCormack et al., 2005). To address this question, stereological cell counts were performed in subregions of the SNc known to differ in their vulnerability in PD (German et al., 1992). True stereological methods require well defined anatomical landmarks to ensure an accurate estimation of the reference volume (West, 2002). However, strict adherence to this criterion precludes the assessment of regional differences in vulnerability, which are a hallmark of the ventral mesencephalic dopaminergic cell groups (German et al., 1988, 1992; Greene et al., 2005). Therefore, we adapted the stereological method by using well defined but arbitrary landmarks to isolate subregions of the SNc. Our results indicate a differential vulnerability to paraquat among nigral dopaminergic neurons with a ventral > medial > lateral gradient. This pattern of neuronal loss in the SNc is reminiscent of the distribution of TH-IR cell loss observed in PD (German et al., 1992), suggesting that paraquat primarily affects those neurons particularly vulnerable to the disease process. These neurons are also more vulnerable to MPTP (German et al., 1992) and to the effects of the weaver mutation (Graybiel et al., 1990), and they contain low levels of the calcium-binding protein calbindin D 28K (German et al., 1992; Liang et al., 1996; McCormack et al., 2006). Results obtained at the level of striatal TH terminals were in accordance with the observed pattern of TH-IR loss in the SNc and with the topographical distribution of nigrostriatal neurons shown in rats (Guyenet and Aghajanian, 1978). The most vulnerable neurons primarily project to the dorsal and medial striatum, regions in which the density of TH-immunoreactive fibers was the most significantly decreased by paraquat exposure. Furthermore, our results indicate that the assessment of the density of TH immunoreactive fibers is more sensitive than OD measurement to detect a moderate loss of nigrostriatal dopaminergic terminals. This result is not surprising when considering the major differences between these methods. OD measurements average areas of staining and background on a 256 grey level image. This method is widely used to detect large differences in immunoreactivity, for example after 6-hydroxydopamine lesions. However, it is notoriously insensitive to detect small changes. For fiber density, the threshold for fiber detection is set in an area of the brain devoid of TH fibers and the area of interest is converted into a two grey levels image (e.g., black and white) by the image analysis system. Staining above threshold will appear black and will be included in the fiber measurement (Bordelon et al., 1999). Therefore, areas devoid of staining are excluded from the measurement and the method is better suited to detect small changes in fiber immunostaining.

To further assess the similarities between neuronal vulnerability to paraquat and to PD, we examined the effects of paraquat on neurons of the LC, a catecholaminergic region also affected in PD (Braak et al., 2003; Halliday et al., 1990; Jellinger, 1991). Paraquat decreased the number of TH-IR neurons in LC but the loss of neurons as measured in Nissl stained sections was only significant by ANOVA, not when post hoc tests were used. These results show for the first time that paraquat can trigger pathological changes in the LC and suggest that, at the dose used in this study, this pesticide induces a modest cell loss but primarily causes a loss of TH immunostaining in this region. It remains to be determined whether this intoxication regimen causes delayed neurodegeneration in LC, or if this could be achieved with subsequent injections of paraquat.

Alterations in LC neurons and the loss of a vulnerable subset of nigrostriatal dopaminergic neurons after repeated paraquat injections in mice, together support the use of this toxin to model PD in vivo, particularly in view of the mechanistic relevance of this environmental toxin to sporadic PD (Hertzman et al., 1990; Liou et al., 1997; Semchuk et al., 1992). However, we were unable to detect any sign of behavioral parkinsonism after paraquat, even though we used a battery of tests that are exquisitely sensitive to nigrostriatal dysfunction in mice (Hwang et al., 2005). The lack of behavioral deficit after paraquat administration is not surprising in view of the small magnitude of neuronal loss and even smaller loss of TH-positive terminals in the striatum. The smaller overall loss of terminals compared with that of cell bodies suggests that some degree of axonal sprouting may have occurred, as previously shown after partial 6-hydroxydopamine lesions (Finkelstein et al., 2000). In addition, it is likely that compensatory mechanisms

(Zigmond et al., 1984) prevented the behavioral manifestations of the small loss of dopaminergic terminals induced by paraquat.

Interactions between paraquat and α-synuclein over-expression

Three other studies have investigated the effects of paraquat or paraquat plus maneb in mice over-expressing α-synuclein (Manning-Bog et al., 2003; Norris et al., 2007; Thiruchelvam et al., 2004). Mice over-expressing human wild-type or A53T α-synuclein under the control of the rat TH promoter were resistant to the administration of paraquat, an effect attributed to an up regulation of hsp70 (Manning-Bog et al., 2003). Conversely, mice over-expressing a doubly mutated human α-synuclein (A30P + A53T) under the control of the rat TH promoter, or A53T α-synuclein under the control of the murine prion promoter were more sensitive to the combined administration of paraquat and maneb (Norris et al., 2007; Thiruchelvam et al., 2004). These studies have not examined the effect of paraquat on motor and sensorimotor deficits as in our study. Furthermore, it is unclear how these data relate to sporadic PD, in which the wild-type rather than the mutated form of α-synuclein accumulates in neurons, and pathology is broadly distributed rather than being restricted to catecholaminergic neurons or involving the spinal cord (Braak et al., 2003).

In the present work, we have examined paraquat toxicity in mice over-expressing wild-type human α-synuclein under the Thy1 promoter. These mice exhibit widespread α-synuclein over-expression in brain (Rockenstein et al., 2002), as well as sensorimotor anomalies (Fleming et al., 2004), abnormal responses to dopaminergic agents (Fleming et al., 2006a), olfactory deficits (Fleming et al., 2006b) and profound synaptic dysfunction in the striatum (Watson et al., 2005; Wu et al., 2005). In contrast to other lines of transgenic mice using the prion promoter, they do not show spinal cord pathology (Fernagut and Chesselet, 2004). Furthermore, the use of the Thy1 promoter results in over-expression of the transgene outside the catecholaminergic neurons, more closely modeling the widespread accumulation of α-synuclein observed in PD (Braak et al., 2003) than with the use of the TH promoter. Finally, they over-express the wild-type protein, which also accumulates in sporadic PD, rather than mutated forms that are only present in very rare familial cases of the disease. Previous findings (Fleming et al., 2004) of sensorimotor anomalies in these mice were reproduced in the present study. These anomalies were not modified by injection of paraquat and similarly, the transgenic mice showed a similar dopaminergic cell loss than the wild-type mice after paraquat administration.

Most pathological studies in α-synuclein over-expressing mice have detected accumulation of the protein histologically without distinguishing between its soluble and insoluble, aggregated forms (Fernagut and Chesselet, 2004; Manning-Bog et al., 2003; Rockenstein et al., 2002). In the present study, we have pretreated sections with proteinase-K to destroy soluble α-synuclein to selectively detect the aggregated form of the protein. This allowed us to confirm the presence of α-synuclein aggregates in many brain regions (Hutson, Fernagut and Chesselet in preparation), including the substantia nigra and LC as reported here. Furthermore, we found that a major difference between saline and paraquat-injected transgenic mice was the marked increase (+91%) in proteinase-K-resistant α-synuclein aggregates in the latter. These proteinase-K-resistant aggregates of α-synuclein were not detected in wild-type mice, either treated with saline or paraquat, despite the fact that our antibody detected mouse α-synuclein. We did not detect an increase in microglia on adjacent sections, indicating that the formation of inclusions was not associated with an inflammatory reaction. As expected, the microglial activation that occurs concomitantly to neurodegeneration was no longer detectable when the mice were sacrificed 2 weeks after the onset of neurodegeneration (McCormack et al., 2002). Together with recent data showing that microglial activation occurs as a priming event leading to neurodegeneration (Purisai et al., 2007), our results indicate that there is no sustained microglial activation in this model.

Abnormal accumulation of α-synuclein in insoluble neuronal or glial inclusions is a pathological hallmark of PD and related synucleinopathies (Spillantini and Goedert, 2000). Previous studies have shown that paraquat can induce an early increase of α-synuclein expression in the substantia nigra, which returns to baseline levels within 1 week (Manning-Bog et al., 2002). It is conceivable that the increase in number and size of protein K-resistant inclusions by paraquat in Thy1-aSYN mice is simply due to an increased level of the protein. However, in vitro studies have also shown that paraquat favors the formation of α-synuclein fibrils (Uversky et al., 2001). In addition, paraquat increases oxidative stress through a redox cycling mechanism (Bonneh-Barkay et al., 2005), which could promote α-synuclein nitration, a modification that increases its resistance to proteolysis (Uversky et al., 2005).

Whatever their mechanisms, the α-synuclein aggregates did not cause neuronal death at the age examined in the transgenic mice, and their increase did not promote cell death in those dopaminergic neurons that are resistant to paraquat. It is of interest that, similar to aggregates of mutated proteins with expanded CAG repeats (Arrasate et al., 2004; Saudou

et al., 1998), aggregates of α-synuclein may be protective rather than deleterious (Chen and Feany, 2005), whereas nonaggregated misfolded forms of the protein may be more toxic (Conway et al., 2001). In humans, α-synuclein pathology is observed in neurons that do not degenerate as well as in regions with marked neuronal loss in PD (Halliday et al., 2006). Although there is no evidence for a direct relationship between α-synuclein inclusions and cell death, these aggregates are clearly indicative of a pathological process in humans (Lee and Trojanowski, 2006; Spillantini and Goedert, 2000).

The marked increase in proteinase-K-resistant inclusions induced by paraquat in α-synuclein over-expressing mice shows that these environmental and genetic manipulations interact in vivo. However, a functional consequence of this interaction was not apparent at the short time point examined. Together with the results of previous studies (Manning-Bog et al., 2003; Norris et al., 2007; Thiruchelvam et al., 2004), our data suggest that synergistic or protective interactions between endogenous (α-synuclein) and environmental (paraquat) risk factors for PD critically depend on their level, duration, and combination. Indeed, it is noteworthy that α-synuclein can exert either a neuroprotective (Leng and Chuang, 2006) or neurotoxic effect (Chen et al., 2006) in vivo. Furthermore, long term over-expression of α-synuclein increases endogenous defense mechanisms, such as the levels of chaperone proteins (Manning-Bog et al., 2003; Cabeza-Arvelaiz et al., in preparation) in young transgenic mice, which could counteract further detrimental effects of toxin injections. It remains possible that the enhanced α-synuclein aggregation in these neurons may signal an increased vulnerability to subsequent insults. Longer term studies with multiple successive toxin exposure will be necessary to test this hypothesis.

Taken together, our data indicate that a genetic predisposition can interact with environmental exposure to promote pathological changes that are relevant to the pathogenesis of PD. Indeed, by targeting the most vulnerable neurons and inducing α-synuclein aggregation, the pathological changes reported in our study are reminiscent of the early stages of PD pathogenesis (Braak et al., 2003; Fearnley and Lees, 1991). Even though there is no direct evidence that increased α-synuclein levels contribute to sporadic PD, the identification of several polymorphisms in the α-synuclein gene associated with increased risk or earlier onset of PD suggest that altered regulation of the α-synuclein gene may be implicated at some time in the disease process (Farrer et al., 2001; Holzmann et al., 2003; Pals et al., 2004). Thus, the increased α-synuclein pathology induced by paraquat in mice that present with elevated α-synuclein levels may represent a mechanism for genetic and environmental interactions in the pathogenesis of PD.

CONCLUSION

The present data strengthen the similarities between the effects of paraquat administration in mice and the neuropathology of PD based on the pattern of affected neurons in the SNc and the vulnerability of LC neurons. They also show that proteinase-K-resistant α-synuclein aggregates are formed in the brain of mice over-expressing α-synuclein and are increased by paraquat exposure, further supporting the hypothesis that one mechanism by which long term exposure to this environmental toxin may increase PD risk is by promoting α-synuclein pathology, a hallmark of sporadic PD (Braak et al., 2006).

ACKNOWLEDGMENTS

REFERENCES

Arrasate M, Mitra S, Schweitzer ES, Segal MR, Finkbeiner S. 2004. Inclusion body formation reduces levels of mutant Huntingtin and the risk of neuronal death. Nature 431:805–810.

Bonneh-Barkay D, Langston WJ, Di Monte DA. 2005. Toxicity of redox cycling pesticides in primary mesencephalic cultures. Antioxid Redox Signal 7:649–653.

Bordelon YM, Chesselet MF. 1999. Early effects of intrastriatal injections of quinolinic acid on microtubule-associated protein-2 and neuropeptides in rat basal ganglia. Neuroscience 93:843–853.

Braak H, Del Tredici K, Rub U, de Vos RA, Steur ENJ, Braak E. 2003. Staging of brain pathology related to sporadic Parkinson's disease. Neurobiol Aging 24:197–211.

Braak H, Bohl JR, Muller CM, Rub U, de Vos RA, Del Tredici K. 2006. Stanley Fahn Lecture 2005: The staging procedure for the inclusion body pathology associated with sporadic Parkinson's disease reconsidered. Mov Disord 21:2042–2051.

Chen L, Feany MB. 2005. α-Synuclein phosphorylation controls neurotoxicity and inclusion formation in a *Drosophila* model of Parkinson disease. Nat Neurosci 8:657–663.

Chen L, Thiruchelvam MJ, Madura K, Richfield EK. 2006. Proteasome dysfunction in aged human α-synuclein transgenic mice. Neurobiol Dis 23:120–126.

Conway KA, Rochet JC, Bieganski RM, Lansbury PT Jr. 2001. Kinetic stabilization of the α-synuclein protofibril by a dopamine-α-synuclein adduct. Science 294:1346–1349.

Di Monte DA, Lavasani M, Manning-Bog AB. 2002. Environmental factors in Parkinson's disease. Neurotoxicology 23:487–502.

Farrer M, Maraganore DM, Lockhart P, Singleton A, Lesnick TG, de Andrade M, West A, de Silva R, Hardy J, Hernandez D. 2001. α-Synuclein gene haplotypes are associated with Parkinson's disease. Hum Mol Genet 10:1847–1851.

Fearnley JM, Lees AJ. 1991. Ageing and Parkinson's disease: Substantia nigra regional selectivity. Brain 114 (Part 5):2283–2301.

Fernagut PO, Chesselet MF. 2004. α-Synuclein and transgenic mouse models. Neurobiol Dis 17:123–130.

Finkelstein DI, Stanic D, Parish CL, Tomas D, Dickson K, Horne MK. 2000. Axonal sprouting following lesions of the rat substantia nigra. Neuroscience 97:99–112.

Fleming SM, Salcedo J, Fernagut PO, Rockenstein E, Masliah E, Levine MS, Chesselet MF. 2004. Early and progressive sensorimotor anomalies in mice overexpressing wild-type human α-synuclein. J Neurosci 24:9434–9440.

Fleming SM, Salcedo J, Hutson CB, Rockenstein E, Masliah E, Levine MS, Chesselet MF. 2006a. Behavioral effects of dopaminergic agonists in transgenic mice overexpressing human wildtype α-synuclein. Neuroscience 142:1245–1253.

Fleming SM, Tetreault N, Masliah E, Chesselet MF. 2006b.Alterations in olfactory function in transgenic mice overexpressing human wild-type α-synuclein. In: 36th Annual Meeting of the Society for Neuroscience, Altanta, October 14–18.

German DC, Dubach M, Askari S, Speciale SG, Bowden DM. 1988. 1-Methyl-4-phenyl-1,2,3,6-tetrahydropyridine-induced Parkinsonian syndrome in *Macaca fascicularis*: Which midbrain dopaminergic neurons are lost? Neuroscience 24:161–174.

German DC, Manaye KF, Sonsalla PK, Brooks BA. 1992. Midbrain dopaminergic cell loss in Parkinson's disease and MPTP-induced Parkinsonism: Sparing of calbindin-D28k-containing cells. Ann N Y Acad Sci 648:42–62.

Graybiel AM, Ohta K, Roffler-Tarlov S. 1990. Patterns of cell and fiber vulnerability in the mesostriatal system of the mutant mouse weaver. I. Gradients and compartments. J Neurosci 10: 720–733.

Greenamyre JT, Hastings TG. 2004. Biomedicine. Parkinson's—Divergent causes, convergent mechanisms. Science 304:1120–1122.

Greene JG, Dingledine R, Greenamyre JT. 2005. Gene expression profiling of rat midbrain dopamine neurons: Implications for selective vulnerability in Parkinsonism. Neurobiol Dis 18:19–31.

Guyenet PG, Aghajanian GK. 1978. Antidromic identification of dopaminergic and other output neurons of the rat substantia nigra. Brain Res 150:69–84.

Halliday GM, Li YW, Blumbergs PC, Joh TH, Cotton RG, Howe PR, Blessing WW, Geffen LB. 1990. Neuropathology of immunohistochemically identified brainstem neurons in Parkinson's disease. Ann Neurol 27:373–385.

Halliday GM, Del Tredici K, Braak H. 2006. Critical appraisal of brain pathology staging related to presymptomatic and symptomatic cases of sporadic Parkinson's disease. J Neural Transm Suppl:99–103.

Hertzman C, Wiens M, Bowering D, Snow B, Calne D. 1990. Parkinson's disease: A case–control study of occupational and environmental risk factors. Am J Ind Med 17:349–355.

Holzmann C, Kruger R, Saecker AM, Schmitt I, Schols L, Berger K, Riess O. 2003. Polymorphisms of the α-synuclein promoter: Expression analyses and association studies in Parkinson's disease. J Neural Transm 110:67–76.

Hwang DY, Fleming SM, Ardayfio P, Moran-Gates T, Kim H, Tarazi FI, Chesselet MF, Kim KS. 2005. 3,4-Dihydroxyphenylalanine reverses the motor deficits in Pitx3-deficient aphakia mice: Behavioral characterization of a novel genetic model of Parkinson's disease. J Neurosci 25:2132–2137.

Jellinger KA. 1991. Pathology of Parkinson's disease. Changes other than the nigrostriatal pathway. Mol Chem Neuropathol 14:153–197.

Lee VM, Trojanowski JQ. 2006. Mechanisms of Parkinson's disease linked to pathological α-synuclein: New targets for drug discovery. Neuron 52:33–38.

Leng Y, Chuang DM. 2006. Endogenous α-synuclein is induced by valproic acid through histone deacetylase inhibition and participates in neuroprotection against glutamate-induced excitotoxicity. J Neurosci 26:7502–7512.

Liang CL, Sinton CM, Sonsalla PK, German DC. 1996. Midbrain dopaminergic neurons in the mouse that contain calbindin-D28k exhibit reduced vulnerability to MPTP-induced neurodegeneration. Neurodegeneration 5:313–318.

Liou HH, Tsai MC, Chen CJ, Jeng JS, Chang YC, Chen SY, Chen RC. 1997. Environmental risk factors and Parkinson's disease: A case–control study in Taiwan. Neurology 48:1583–1588.

Manning-Bog AB, McCormack AL, Li J, Uversky VN, Fink AL, Di Monte DA. 2002. The herbicide paraquat causes up-regulation and aggregation of α-synuclein in mice: Paraquat and α-synuclein. J Biol Chem 277:1641–1644.

Manning-Bog AB, McCormack AL, Purisai MG, Bolin LM, Di Monte DA. 2003. α-Synuclein overexpression protects against paraquat-induced neurodegeneration. J Neurosci 23:3095–3099.

Matsuura K, Kabuto H, Makino H, Ogawa N. 1997. Pole test is a useful method for evaluating the mouse movement disorder caused by striatal dopamine depletion. J Neurosci Methods 73:45–48.

McCormack AL, Thiruchelvam M, Manning-Bog AB, Thiffault C, Langston JW, Cory-Slechta DA, Di Monte DA. 2002. Environmental risk factors and Parkinson's disease: Selective degeneration of nigral dopaminergic neurons caused by the herbicide paraquat. Neurobiol Dis 10:119–127.

McCormack AL, Atienza JG, Johnston LC, Andersen JK, Vu S, Di Monte DA. 2005. Role of oxidative stress in paraquat-induced dopaminergic cell degeneration. J Neurochem 93:1030–1037.

McCormack AL, Atienza JG, Langston JW, Di Monte DA. 2006. Decreased susceptibility to oxidative stress underlies the resistance of specific dopaminergic cell populations to paraquat-induced degeneration. Neuroscience 141:929–937.

Norris EH, Uryu K, Leight S, Giasson BI, Trojanowski JQ, Lee VM. 2007. Pesticide exposure exacerbates α-synucleinopathy in an A53T transgenic mouse model. Am J Pathol 170:658–666.

Pals P, Lincoln S, Manning J, Heckman M, Skipper L, Hulihan M, Van den Broeck M, De Pooter T, Cras P, Crook J, Van Broeckhoven C, Farrer MJ. 2004. α-Synuclein promoter confers susceptibility to Parkinson's disease. Ann Neurol 56:591–595.

Purisai MG, McCormack AL, Cumine S, Li J, Isla MZ, Di Monte DA. 2007. Microglial activation as a priming event leading to paraquat-induced dopaminergic cell degeneration. Neurobiol Dis 25:392–400.

Rockenstein E, Mallory M, Hashimoto M, Song D, Shults CW, Lang I, Masliah E. 2002. Differential neuropathological alterations in transgenic mice expressing α-synuclein from the platelet-derived growth factor and Thy-1 promoters. J Neurosci Res 68:568–578.

Sanghera MK, Manaye K, McMahon A, Sonsalla PK, German DC. 1997. Dopamine transporter mRNA levels are high in midbrain neurons vulnerable to MPTP. Neuroreport 8:3327–3331.

Saudou F, Finkbeiner S, Devys D, Greenberg ME. 1998. Huntingtin acts in the nucleus to induce apoptosis but death does not correlate with the formation of intranuclear inclusions. Cell 95:55–66.

Semchuk KM, Love EJ, Lee RG. 1992. Parkinson's disease and exposure to agricultural work and pesticide chemicals. Neurology 42:1328–1335.

Spillantini MG, Goedert M. 2000. The α-synucleinopathies: Parkinson's disease, dementia with Lewy bodies, and multiple system atrophy. Ann N Y Acad Sci 920:16–27.

Thiruchelvam MJ, Powers JM, Cory-Slechta DA, Richfield EK. 2004. Risk factors for dopaminergic neuron loss in human α-synuclein transgenic mice. Eur J Neurosci 19:845–854.

Uversky VN, Li J, Fink AL. 2001. Pesticides directly accelerate the rate of α-synuclein fibril formation: A possible factor in Parkinson's disease. FEBS Lett 500:105–108.

Uversky VN, Yamin G, Munishkina LA, Karymov MA, Millett IS, Doniach S, Lyubchenko YL, Fink AL. 2005. Effects of nitration on the structure and aggregation of α-synuclein. Brain Res Mol Brain Res 134:84–102.

van der Putten H, Wiederhold KH, Probst A, Barbieri S, Mistl C, Danner S, Kauffmann S, Hofele K, Spooren WP, Ruegg MA, Lin S, Caroni P, Sommer B, Tolnay M, Bilbe G. 2000. Neuropathology in mice expressing human α-synuclein. J Neurosci 20:6021–6029.

Watson JB, Chesselet MF, Masliah E, Levine MS. 2005. Enhancement of striatal synaptic plasticity in α-synuclein overexpressing mice. In: 35th Annual Meeting of the Society for Neuroscience, Washington, DC, November 12–16.

West MJ. 2002. Design-based stereological methods for counting neurons. Prog Brain Res 135:43–51.

West MJ, Slomianka L, Gundersen HJ. 1991. Unbiased stereological estimation of the total number of neurons in thesubdivisions of the rat hippocampus using the optical fractionator. Anat Rec 231:482–497.

Wu N, Cepeda C, Masliah E, Levine MS. 2005.Abnormal glutamate and dopamine receptor function in the striatum of α-synuclein overexpressing mice. In: 35th Annual Meeting of the Society for Neuroscience, Washington, DC, November 12–16.

Zigmond MJ, Acheson AL, Stachowiak MK, Stricker EM. 1984. Neurochemical compensation after nigrostriatal bundle injury in an animal model of preclinical Parkinsonism. Arch Neurol 41:856–861.